Planar SIW cavity-backed antenna loaded with slots for multiband operations

R. Samson Daniel[1]

Abstract

A low-profile substrate integrated waveguide (SIW) cavity-backed antenna loaded with slots is presented for multiband operations. This antenna is designed by loading a rectangular and square-shaped slot onto a rectangular SIW cavity for multiband radiation. The slots are created inside the rectangular cavity to induce a hybrid mode (i.e. $TE_{110} + TE_{120}$), which supports to radiate a lower resonance frequency. The rectangular slot is used to excite TE_{120} mode at 5.21 GHz, while square-shaped slot excites hybrid mode at 2.21 GHz. This hybrid mode is obtained by coupling the cavity modes TE_{110} and TE_{120} through the metallized via-holes. The designed antenna yields multiband response owing to resonant slots when governed by the inset microstrip feedline. The operating modes are explained with the help of mode theory mechanism. The fabricated antenna comprises with dimensions $30 \times 30 \times 1.6$ mm^3, which is printed on a low-cost Flame Retardant-4 dielectric substrate. To verify the simulated counterparts, the fabricated antenna has been tested, which offers a fractional bandwidth of 6.9% (2.10–2.25 GHz) in the hybrid mode at 2.18 GHz, 8.4% (3.35–3.64 GHz) in the TE_{110} mode at 3.45 GHz and 10.8% (5.04–5.61 GHz) in the TE_{120} mode at 5.26 GHz with suitable far-field pattern.

Keywords Hybrid mode · Multiband · SIW · Rectangular slot · Square-shaped slot

1 Introduction

Microstrip patch antennas have concentrated in advanced wireless communication systems due to low-profile, low cost and integrate with MIC circuits [1]. These antennas are essential for wireless devices such as mobile phones, modem and biomedical devices. However, it suffers from narrow resonance and lower gain values [2]. Numerous design methods have been deliberated for achieving multiband such as fractal configurations [3], metamaterial [4] and loading slots [5].

In a recent scenario, SIW antennas have been evolving as an eminent contributor in millimetre wave applications owing to planar configurations, compact size and better radiation characteristics. Several antenna designers have encouraged SIW antennas in microwave communications due to the high gain [6], circular polarization [7] and broad bandwidth [8]. The geometry of SIW antenna provides a shielded medium for avoiding spurious radiation, which is improved the overall performance of the antenna. SIW methodologies have been used in inventing power divider [9], beam forming network [10], filters [11] and electrically small antennas [12]. SIW cavity loaded with bow-tie slot [13], modified triangular ring slot [14] and circular ring slot [15] have been realized for multiband abilities. An octa-star slot-loaded circular-shaped SIW cavity-backed antenna with coax probe feed is designed for broadband characteristics [16]. SIW technologies are feasible for constructing a technique to develop modern equipment such as photonic integrated circuits, broadcasting, radar and telecommunication applications.

In this article, a design of slotted SIW cavity-backed antenna with inset feed is demonstrated. The designed antenna uses suitable position of a rectangular and square-shaped slot to influence the current distribution at the top plane for radiating multiband and 83% of the size reduction. It has an electrical size of $0.221 \lambda_0 \times 0.221 \lambda_0 \times 0.0117 \lambda_0$, where λ_0 is the free space wavelength at $f_0 = 2.21$ GHz. The proposed method is beneficial to identify devices for telecommunication and wireless applications owing to planar configuration, lower losses, low-profile and high power

✉ R. Samson Daniel
  samson.rapheal@gmail.com

1 Department of Electronics and Communication
   Engineering, K. Ramakrishnan College of Engineering,
   Samayapuram, Tiruchirappalli, Tamil Nadu, India

capability. The proposed antenna possesses the benefits of multiband attributes along with compact size compared with earlier published work [6–8, 12–15].

2 Proposed antenna design and working principle

The designed antenna is developed from a dual-band rectangular SIW cavity-backed resonator as explained in the Prototype 1 of Fig. 1. In Prototype 2, a rectangular slot is loaded in proximity to the right side cavity. It governs the electric field of the rectangular cavity and yields modified upper resonance frequency (i.e. TE_{120}). Thus, the rectangular slot is capable of governing upper resonance frequency of the proposed antenna. The square-shaped slot with conducting strip is introduced in the centre of the cavity to create a hybrid mode for constructing lower resonance frequency as depicted in Fig. 1 of Prototype 3. These slots are excited by 50 Ω inset feedline for generating the resonance frequencies of 2.21 GHz, 3.45 GHz and 5.21 GHz.

The equivalent circuit of the proposed SIW antenna is described in Fig. 2. The LC model is explained for

rectangular SIW cavity, rectangular slot and square-shaped slot with conducting strip. The inductances are governed by via arrangement and it is indicated by L_{vias}. The coupling capacitance (C_c) and connection of inductances (L_c) form between the SIW cavity and planar transmission line, where C_r and L_r are the parasitic capacitance and inductance of the transmission line, respectively. The lumped components (R_1, L_1, C_1) are caused by rectangular slot and lumped components (R_2, L_2, C_2) are caused by square-shaped slot with conducting strip. The perspective view of the designed antenna is illustrated in Fig. 3, and its geometrical values are listed in Table 1.

The configurations of the designed antenna are simulated using HFSS V.14.0 EM tool. The simulated input reflection coefficients of the Prototype 1, Prototype 2 and Prototype 3 are shown in Fig. 4. The conventional rectangular SIW cavity-backed antenna is fashioned using metallic vias and the SIW rules pitch distance (s) and diameter (d) of the metallic vias have been maintained $d/s \geq 0.5$ and $d/\lambda_0 \leq 0.1$ for preventing leakage of EM energy. The length and width of the rectangular cavity resonator have been estimated using [12]:
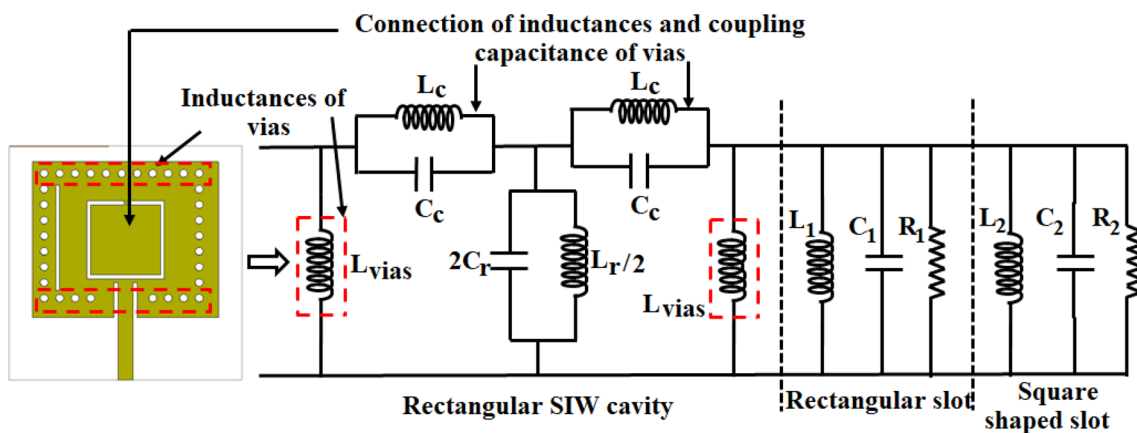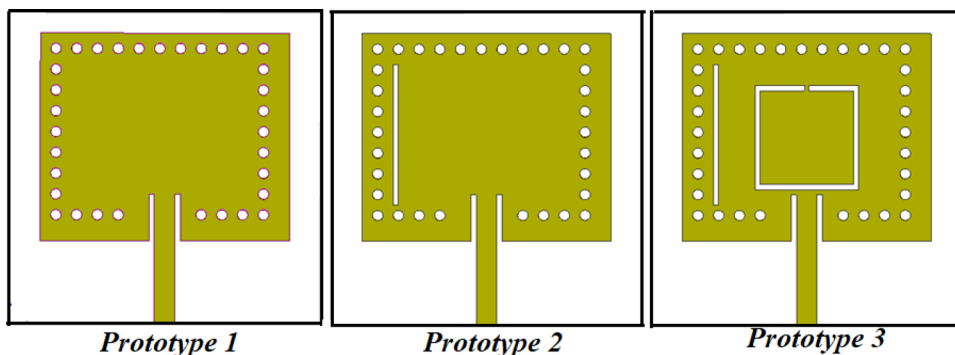

Fig. 1 Prototype configurations
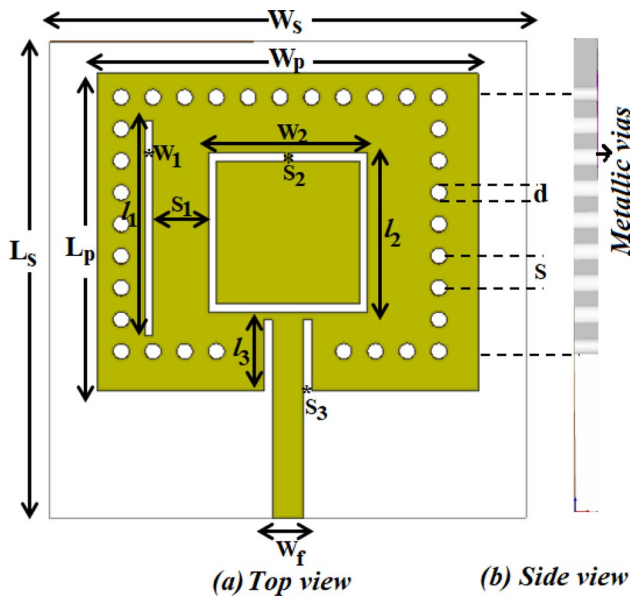

Fig. 2 Equivalent circuit topology

Fig. 3 Perspective view of the designed antenna

Fig. 4 S_{11}(dB) of the design configurations

Table. 1 Geometrical values of the proposed antenna

Parameters	Dimensions (mm)
W_s	30
L_s	30
W_p	24
L_p	20
l_1	13.5
w_1	0.5
l_2	10
w_2	10
S_1	3.5
S_2	0.4
S_3	0.5
d	1
S	2

$$f_r(TE_{mnp}) = \frac{c}{2\sqrt{\varepsilon_r}}\sqrt{\left(\frac{m}{L}\right)^2 + \left(\frac{n}{W}\right)^2 + \left(\frac{p}{h}\right)^2} \quad (1)$$

where L is the length of the SIW cavity, W is the width of the SIW cavity, c is the velocity of light, ε_r dielectric constant of the substrate, m, n, p are mode indices. Thus, the Prototype 1 produces two cavity modes TE_{110} at 3.53 GHz and TE_{120} at 5.83 GHz. When the rectangular slot is introduced (Prototype 2), the cavity mode TE_{120} gets adjusted and offers the modified TE_{120} mode at 5 GHz without affecting 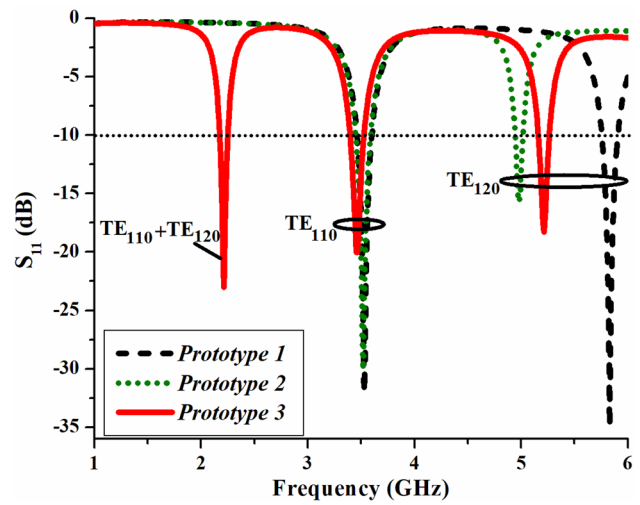TE_{110} mode. Here, the length of the rectangular slot can be predicted to the half the resonant wavelength (i.e. $l_1 = \lambda_g/2$). Therefore:

$$f_r = \frac{c}{2l_1\sqrt{\varepsilon_r}} = \frac{3 \times 10^8}{2 \times 13.5 \times 10^{-3}\sqrt{4.4}} = 5.29 \text{ GHz} \quad (2)$$

where ε_r is the dielectric constant of FR-4 substrate. It reveals that rectangular slot creates resonance at 5.29 GHz, which is verified with simulated resonance at 5 GHz.

In Prototype 3 (proposed antenna), a square-shaped slot with conducting strip is introduced, which couples the cavity mode TE_{110} with modified TE_{120} mode and creates hybrid mode (i.e. $TE_{110} + TE_{120}$) at 2.21 GHz near to the cavity mode TE_{110}. Also, the modified TE_{120} mode is shifted from 5 to 5.21 GHz and TE_{110} mode slightly shifts towards the downward and resonates at 3.45 GHz. This hybrid mode resonance frequency has been estimated using [17]:

$$L_1 = 2l_2 + w_2 + 2\Delta l_{eff} \quad (3)$$

where the fringe field depth Δl_{eff} is equal to the FR-4 substrate thickness ($h = 1.6$ mm), $l_2 = 10$ mm and $W_1 = 10$ mm is the length and width of the square-shaped slot. Therefore, $L_1 = 33.2$ mm and the resonant frequency is given by:

$$f_r = \frac{c}{2L_1\sqrt{\varepsilon_r}} = \frac{3 \times 10^8}{2 \times 33.2 \times 10^{-3}\sqrt{4.4}} = 2.15 \text{ GHz}$$

From this equation, it is found that the square-shaped slot offers resonance at 2.15 GHz, which matches with simulated resonant frequency of 2.21 GHz.

3 Operating mechanism

The electric field distribution and corresponding vector magnetic field of the SIW cavity-backed antenna without slot loading are depicted in Fig. 5a–b, which explains the field distribution for TE_{110} and TE_{120} cavity modes. The real part input impedance of the design configurations is represented in Fig. 6. It is perceived that loading of the slots greatly influences cavity modes (TE_{110} and TE_{120}) and offers a hybrid mode at 2.21 GHz. Similarly, SIW cavity resonator governs the cavity mode TE_{110} at 3.45 GHz and rectangular slot governs the upper cavity mode TE_{120} at 5.21 GHz. The same can be inferred from electric field distribution of SIW cavity-backed antenna loaded with slots, which describes in Fig. 7a–c, respectively. Thus, the square-shaped slot with conducting strip splits the resonator into two components, including extended outer aperture and parasitic inner square aperture. The maximum electric field is concentrated in the parasitic inner square aperture at 2.21 GHz (hybrid mode),
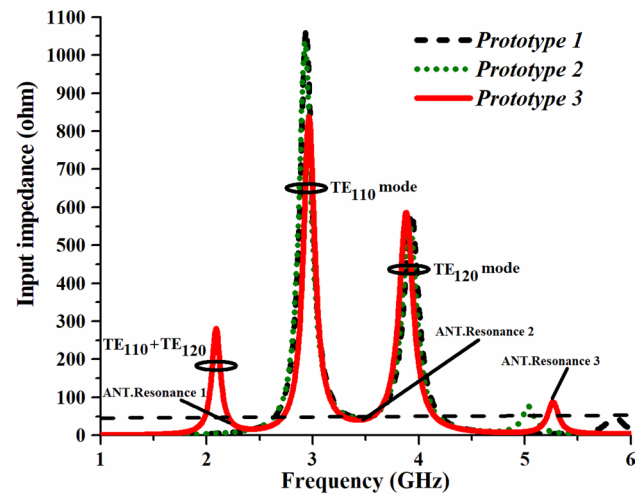

Fig. 6 Real part input impedance of the design configurations

whereas the maximum electric field of the cavity mode TE_{110} at 3.45 GHz is concentrated in the extended outer aperture
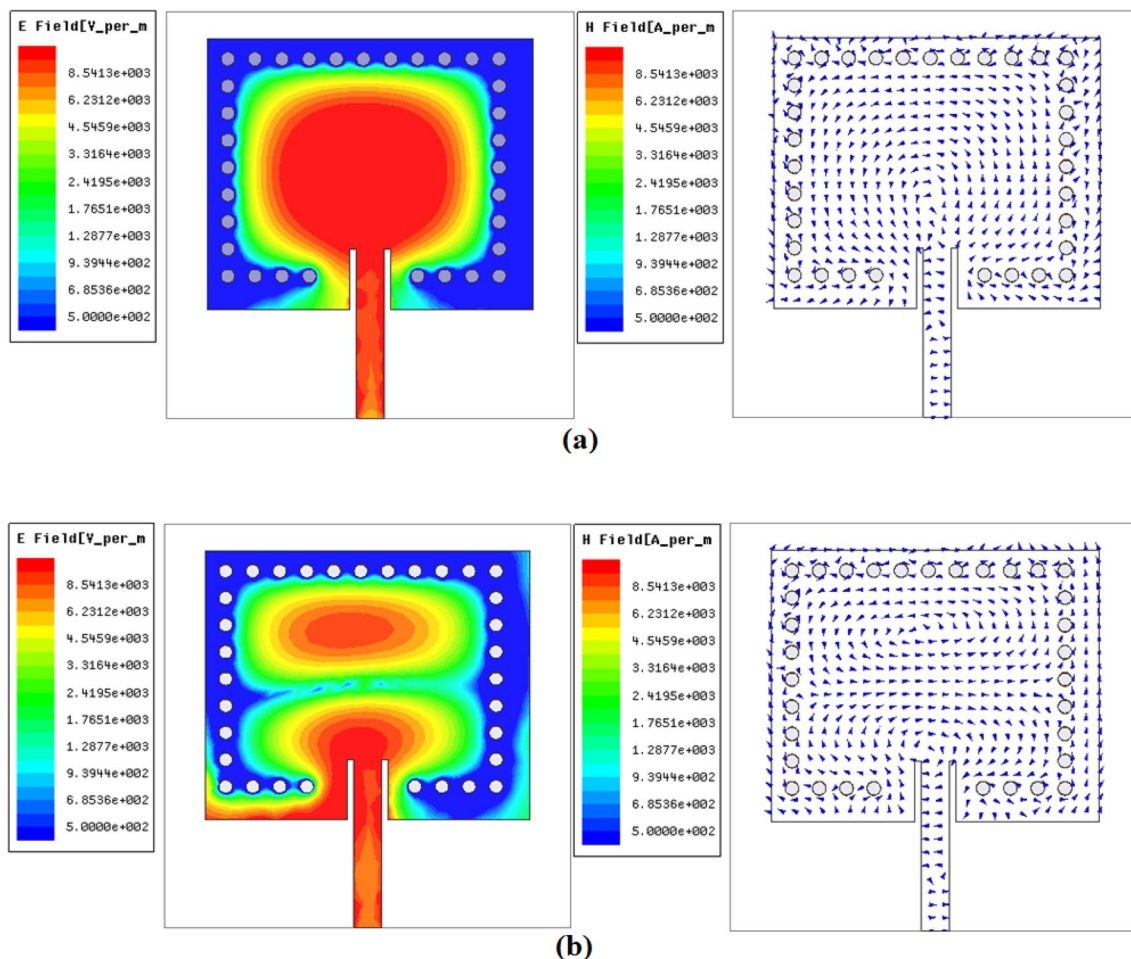

(a)

(b)

Fig. 5 Electric field distribution and corresponding vector magnetic field of the SIW cavity-backed antenna without slot at **a** 3.53 GHz (TE_{110} mode) and **b** 5.83 GHz (TE_{120} mode)
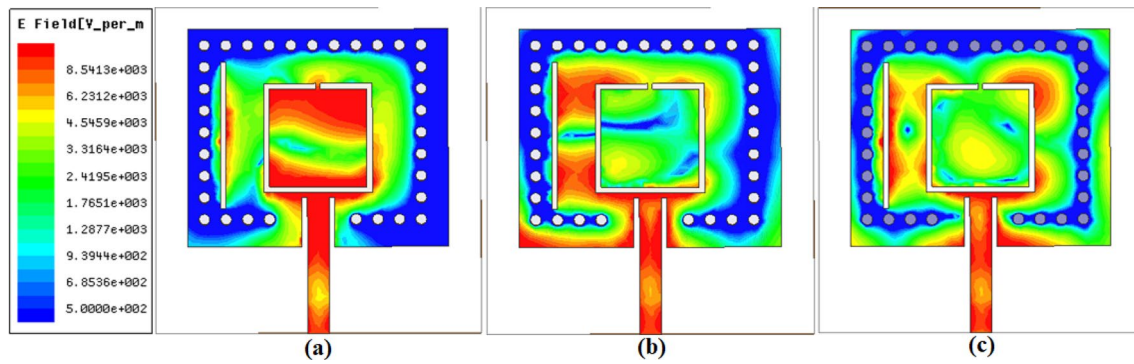
Fig. 7 Electric field distributions of SIW cavity-backed antenna loaded with slots at **a** 2.21 GHz, **b** 3.45 GHz and **c** 5.21 GHz
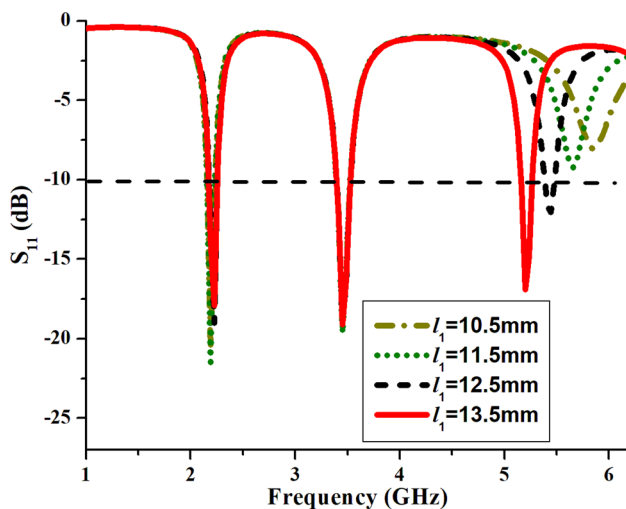
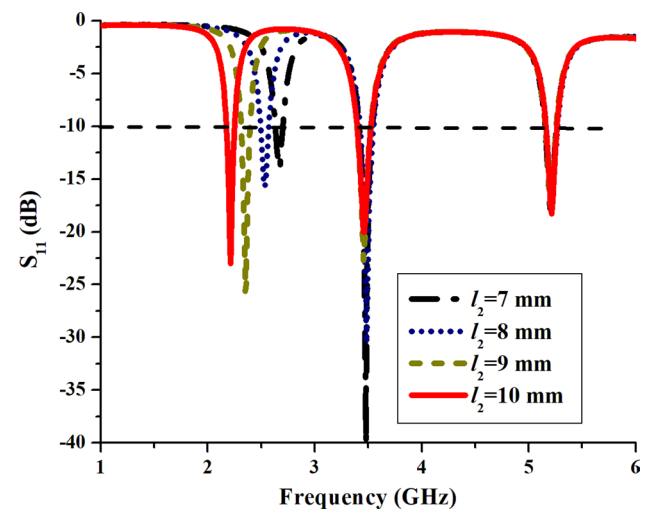

Fig. 8 Effect on length of the rectangular slot (l_1)

Fig. 9 Effect on length of the square-shaped slot (l_2)

of the cavity. In the upper resonance frequency of 5.21 GHz (i.e. TE_{120} mode), the maximum field intensity has been exposed along the rectangular slot at the extended outer aperture. In above specified case, the minimum field intensity arrives on the square-shaped slot and it is employed to build lower resonance frequency.

4 Parametric study

To observe the results of geometrical parameters on the resonance behaviour, a parametric analysis has been conducted. The characteristics of operating frequencies with rectangular slot length (l_1), square-shaped slot length (l_2) and square-shaped slot with strip and without strip are explained in this section. The effect on the length of the rectangular slot (l_1) is discussed in Fig. 8. This evaluation describes that the upper resonance frequency is significantly influences on the rectangular slot(l_1). As the length

of rectangular slot increases, the upper resonance frequency (i.e. TE_{120} mode) decreases and it supports power to be delivered into the load for the first and middle band due to coupling between the SIW cavity resonator and rectangular slot. Hence, optimum value $l_1 = 13.5$ mm is opted for the designed antenna. The length of the square-shaped slot (l_2) illustrates an eminent impact on hybrid mode, as shown in Fig. 9. As the length of the square-shaped slot (l_2) increases, the lower resonance frequency equivalent to hybrid mode decreases, while TE_{110} and TE_{120} modes are same. Therefore, the maximum possible value $= l_2 10$ mm has been selected for optimum performance of the antenna.

Similarly, the effect on square-shaped slot with and without metallic strip is explained in Fig. 10. The square-shaped slot without metallic strip generates an extra shunt inductance owing to the nested cavity structure, which disturbs the resonance behaviour (both hybrid and TE_{110} mode) of the extended outer aperture of the cavity. To balance this, series capacitance is added by creating a
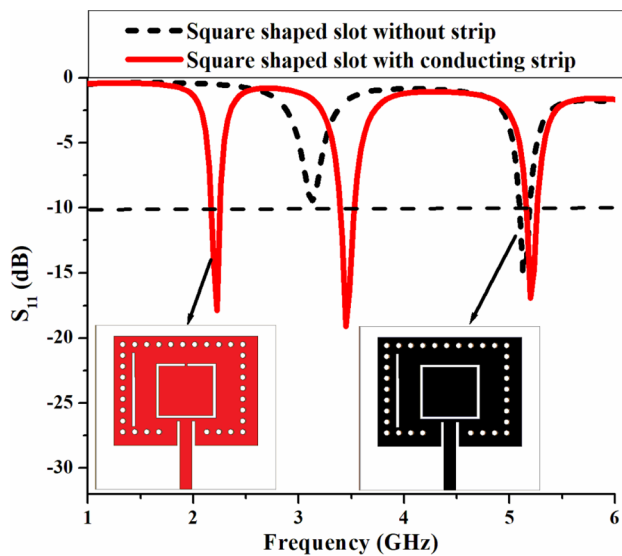
Fig. 10 Effect of metallic strip on square-shaped slot

metallic strip on a square-shaped slot. Thus, the square-shaped slot with metallic strip induces hybrid mode at 2.21 GHz and TE_{110} mode at 3.45 GHz.

Finally, the proposed antenna design steps have been summarized as follows:

- Estimate the length (L) and width (W) of the rectangular cavity [12].
- Introduce a rectangular slot of length l_1 with suitable location as illustrated in Fig. 1 (Prototype 2) to resonate a modified TE_{120} mode. Tune the length to excite better

impedance matching in the upper resonance frequency at 5.21 GHz.

- Place a square-shaped slot of length l_2 as depicted in Fig. 1 (Prototype 3) to excite hybrid mode (TE_{110}+ TE_{120}) at 2.21 GHz.
- Create a metallic strip (series capacitance) on square-shaped slot to balance an extra shunt inductance owing to the nested cavity structure. Thus, the suitable position of metallic strip, the cavity mode TE_{110} and modified TE_{120} mode can be combined to radiate a lower resonance frequency and also, better impedance matching is achieved.
- Finally, the length of the slots and cavity dimensions can be attuned to adjust the resonance behaviour.

5 Measured results and discussion

The structure of the fabricated antenna is shown in Fig. 11. S_{11}(dB) characteristics of the fabricated antenna are experimentally confirmed with the help of Anritsu Vector Network Analyser MS2027C. The measured S_{11}(dB) and gain performances of the designed antenna are correlated in Fig. 12, which is inferred that simulated counterpart agrees with measured results. The simulated S_{11}(dB) exhibits a—10 dB impedance bandwidth of 90 MHz (2.17–2.26 GHz) at 2.21 GHz, 120 MHz (3.41–3.53 GHz) at 3.45 GHz and 100 MHz (5.18–5.28 GHz) at 5.21 GHz, while the experimental bandwidth reveals 150 MHz (2.10–2.25 GHz) at 2.18 GHz, 290 MHz (3.35–3.64 GHz) at 3.45 GHz and 570 MHz (5.04–5.61 GHz) at 5.26 GHz. Due to perfect matched termination, the measured result provides better

Fig. 11 Fabricated antenna: **a** Top view, **b** Bottom view
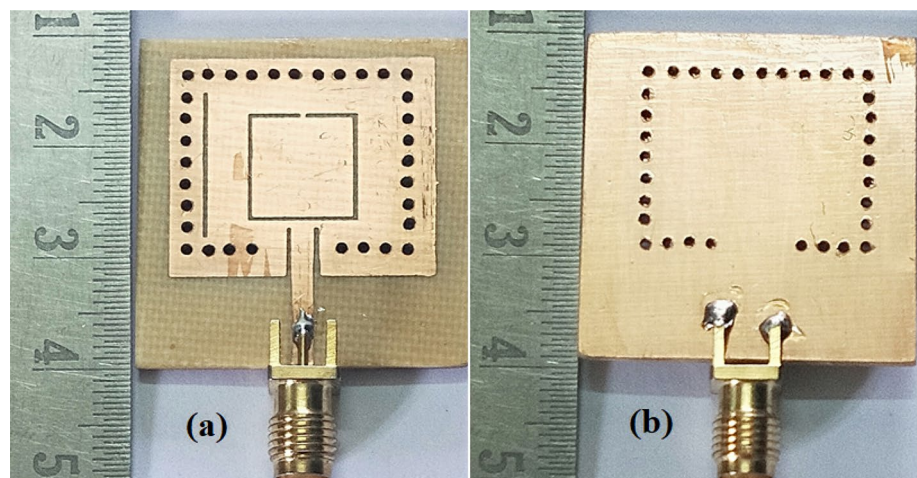
impedance bandwidth when the inset microstrip feedline is excited. However, a small variation between the simulated and tested S_{11}(dB) values is ascertained which may be influenced by the fabrication defectiveness, thick soldering SMA connector and measurement inaccuracy. Moreover, the gain transfer technique has been used to compute the peak gains of the antenna, which is measured by standard horn model 'HRN0118'. It offers a measured peak gain of 3.53 dBi at 2.18 GHz, 5.14 dBi at 3.45 GHz and 5.76 dBi at 5.26 GHz.

The normalized field patterns of the elevation plane (YZ, $\phi = 90°$) and azimuthal plane (XZ, $\phi = 0°$) of the fabricated geometry have been tested in an anechoic chamber. The correlation between the simulated and experimental far-field patterns at 2.18 GHz, 3.45 GHz and 5.26 GHz is depicted in Fig. 13a−c. It explains a broadside direction at 2.18 GHz as illustrated in Fig. 13a, which is influenced owing to the cancellation of the equal magnitude of the electric field intensity and in-phase across the rectangular slot. However, the field patterns at 3.45 GHz and 5.26 GHz are unidirectional and concerned with broadside direction, as shown in Fig. 13b and c. The proposed configuration reveals low back-lobe radiation owing to the cavity-backed structural alignment. Furthermore, the designed antenna supports the integrated benefits of conventional antenna (i.e. reduced back-lobe radiation, better gain), and planar configurations (i.e. compact size and cost-effective fabrication using printed circuit board) (Fig. 13).

The proposed SIW antenna has been correlated with existing SIW antennas indexed in reference is detailed in Table 2. It can be recognized that the proposed SIW geometry yields multiband characteristics with minimum aperture area for UMTS, WiMAX and WLAN applications.

The proposed SIW cavity-backed antenna has focused on the multiband radiation. Multivariate chemometric model [18] can be useful to explore the best experimental conditions for the proper functioning device behaviour, which is used to prevent measurement inaccuracy. In future, the proposed antenna can be carried out with lithium batteries [19, 20] for energy storage and shifts the resonant frequency in the lower frequency region.

6 Conclusion

A compact SIW cavity-backed antenna loaded with slots is presented for multiband applications. The combination of rectangular slot and square-shaped slot with metallic strip is used to create lower hybrid mode proximity to the TE_{110} cavity mode. The performance of the designed antenna is explained by parametric analysis. The designed antenna has an electrical size of $0.221\,\lambda_0 \times 0.221\,\lambda_0 \times 0.0117\,\lambda_0$. The fabricated antenna has been confirmed by testing radiation characteristics. The simulated and tested results depict a good agreement. An experimental planar configuration offers reasonable gain, lower cross-polarization and unidirectional pattern for 2.21 GHz UMTS, 3.45 GHz WiMAX and 5.21 GHz WLAN applications while maintaining compact antenna geometry.
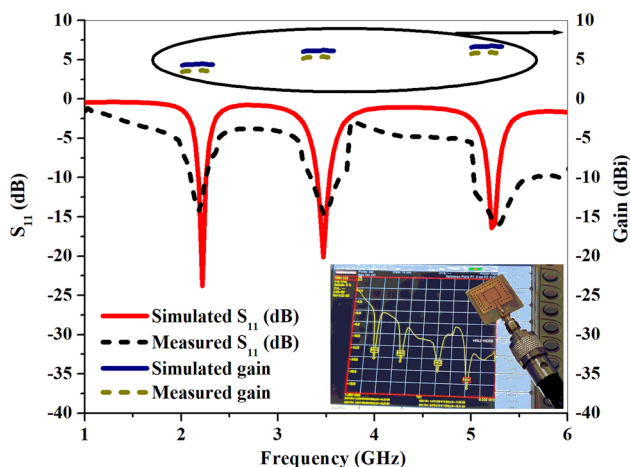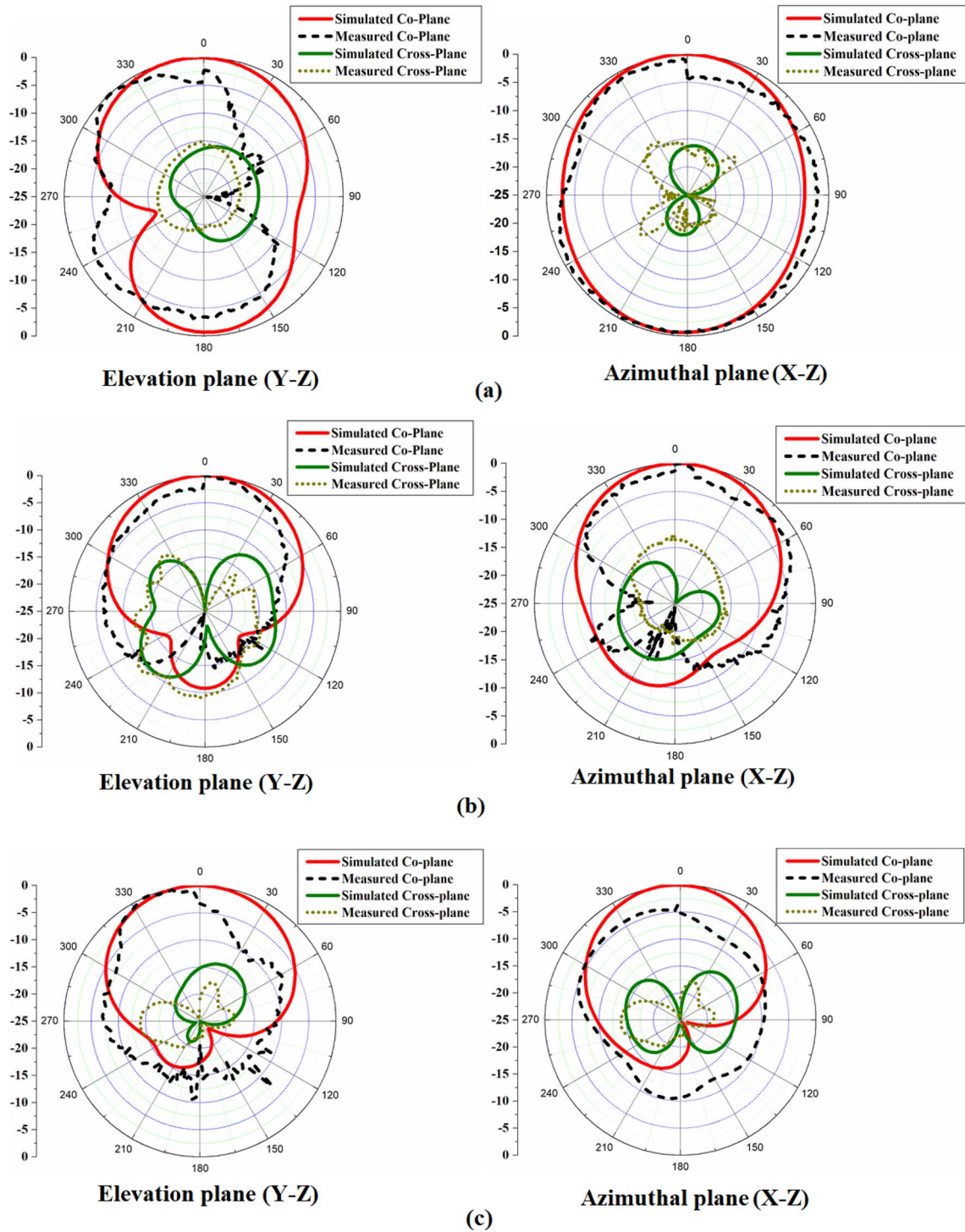

Fig. 12 S_{11}(dB) and gain plots

Fig. 13 Far-field patterns at **a** 2.18 GHz, **b** 3.45 GHz and **c** 5.26 GHz

Table 2 Comparative analysis of the proposed antenna with earlier published work

Ref	Year	Patch detail	Substrate dimensions L×W (mm²)	Resonance frequency (GHz)	Impedance bandwidth (MHz)
[13]	2016	SIW cavity-backed antenna loaded bow-tie slot	37×28.7	8.13 and 10.4	600 MHz (7.98–8.57 GHz) 888 MHz (9.72–10.6 GHz)
[14]	2018	SIW antenna with pair of triangular complementary split ring slots	30×45	8.6 and 13.3	200 MHz (8.70–8.50 GHz) 810 MHz (13.03–13.84 GHz)
[6]	2018	SIW antenna loaded with rectangular slot	78×22	9.5	700 MHz
[7]	2018	SIW cavity-backed square ring slot antenna	39.8×22.28	10, 10.8 and 11.54	1750 MHz (9.92–11.67 GHz)
[8]	2018	SIW cavity-backed triangular ring slotted antenna	32.7×15.4	14.6 and 15.7	2060 MHz(14.43–16.49 GHz)
[15]	2019	Rectangular and circular SIW cavities loaded with circular slots	48×52	5.2 and 5.8	310 MHz (5.04–5.35 GHz) 190 MHz (5.73–5.92 GHz)
[12]	2020	SIW antenna with slots and two metallic vias	42×24	5.7 and 5.85	340 MHz (5.57–5.91 GHz
Proposed antenna		SIW cavity-backed antenna loaded with slots	30×30	2.21, 3.45 and 5.21	80 MHz (2.17–2.25 GHz) 140 MHz (3.39–3.53 GHz) 110 MHz (5.16–5.27 GHz)

References

1. B. Tiwari, S.H. Gupta, V. Balyan, Design and comparative analysis of compact flexible UWB antenna using different substrate materials for WBAN applications. Appl. Phys. A Mater. Sci. Process. **126**, 858 (2020)
2. B. Murugeshwari, R. Samson Daniel, S. Raghavan, A compact dual band antenna based on metamaterial-inspired split ring structure and hexagonal complementary split-ring resonator for ISM/WiMAX/WLAN applications. App. Phys. A Mater. Sci. Process. **125**, 628 (2019)
3. R. Chen, S. Li, Gu. Chendong, S. Anwar, Bo. Hou, Y. Lai, Electromagnetic characteristics of Hilbert curve-based metamaterials . Appl. Phys. A Mater. Sci. Process. **117**, 445–450 (2014)
4. R. Samson Daniel, R. Pandeeswari, S. Raghavan, Dual-band monopole antenna loaded with ELC metamaterial resonator for WiMAX and WLAN applications. Appl. Phys. A Mater. Sci. Process. **124**, 570 (2018)
5. E.A. Mohammad, H.A. Rahim, P.J. Soh, Dual-band circularly polarized textile antenna with split-ring slot for off-body 4G LTE and WLAN applications. Appl. Phys. A Mater. Sci. Process. **124**, 568 (2018)
6. S. Mukherjee, A. Biswas, Design of planar high-gain antenna using SIW cavity hybrid mode. IEEE Trans. Antennas Propag. **66**(2), 972–977 (2018)
7. A. Kumar, S. Raghavan, SIW cavity-backed circularly polarized square ring slot antenna with wide axial-ratio bandwidth. AEU Int J Electron C **94**, 122–127 (2018)
8. A. Kumar, S. Raghavan, Broadband SIW cavity-backed triangular-ring-slotted antenna for Ku -band applications. AEU Int. J. Electron. C **87**, 60–64 (2018)
9. R.V. Gatti, R. Rossi, Hermetic broadband 3-db power divider/combiner in substrate-integrated waveguide (SIW) technology. IEEE Trans. Microw. Theory Tech. **66**(6), 3048–3054 (2018)
10. M.M. Pezhman, A.A. Heidari, A. Ghafoorzadeh-Yazdi, Compact three-beam antenna based on SIW multi-aperture coupler for 5G applications. AEU Int. J. Electron. C **123**, 153302 (2020)
11. L.-F. Shi, C.-Y. Sun, S. Chen, G.-X. Liu, Y.-F. Shi, Dual-band substrate integrated waveguide bandpass filter based on CSRRs and multimode resonator. Int. J. RF Microw. Comput. Aided Eng. **28**, e21412 (2018)
12. D. Chaturvedi, SIW cavity-backed 24° inclined-slots antenna for ISM band application. Int J RF Microw Comput Aided Eng. **30**, e22160 (2020)
13. S. Mukherjee, A. Biswas, Design of dual band and dual-polarised dual band SIW cavity backed bow-tie slot antennas. IET Microw. Antennas Propag. **10**(9), 1002–1009 (2016)
14. A. Kumar, M. Saravanakumar, S. Raghavan, Dual-frequency SIW-based cavity backed antenna. AEU Int. J. Electron. C **97**, 195–201 (2018)
15. D. Chaturvedi, A. Kumar, S. Raghavan, A nested SIW cavity-backing antenna for Wi-Fi/ISM band applications. IEEE Trans. Antennas Propag. **67**(4), 2775–2780 (2019)
16. A. Kumar, Wideband circular cavity-backed slot antenna with conical radiation patterns. Microw. Opt. Technol. Lett. 1–8 (2020)
17. A. Kunwar, A. KumarGautam, K. Rambabu, Design of a compact U-shaped slot triple band antenna for WLAN/WiMAX applications. AEU Int. J. Electron. C **71**, 82–88 (2017)
18. B. Miccoli, V. Cauda, A. Bonanno, A. Sanginario, K. Bejtka, F. Bella, M. Fontana, D. Demarchi, One-dimensional ZnO/Gold junction for simultaneous and versatile multisensing measurements. Sci. Rep. **6**, 29763 (2016)
19. G. Pianaa, F. Bellaa, F. Geobaldob, G. Meligranaa, C. Gerbaldi, PEO/LAGP hybrid solid polymer electrolytes for ambient temperature lithium batteries by solvent-free, "one pot" preparation. J. Energy Storage **26**, 100947 (2019)
20. F. Bella, A.B. Muñoz-García, F. Colo, Combined structural, chemometric, and electrochemical investigation of vertically aligned TiO$_2$ nanotubes for na-ion batteries. ACS Omega **3**, 8440–8450 (2018)